PAMM · Proc. Appl. Math. Mech. **6**, 241–242 (2006) / **DOI** 10.1002/pamm.200610101

Finite strain model for contact interface in forming processes

Mariela Luege* and **Bibiana M. Luccioni**

Instituto de Estructuras, Universidad Nacional de Tucumán, CONICET
Av. Roca 1800, S.M. de Tucumán, 4000 Tucumán, Argentina

A phenomenological rate and state-variable friction law for the continuous sliding under lubricated and dry conditions, as it occurs in metal forming processes, is presented in this paper. The contact model is developed within the framework of continuum thermodynamics of irreversible processes with internal variables and for large strains assuming the contact area as a material surface. The model reproduces the experimental boundary friction map obtained by Luengo et al [1].

1 Introduction

Experimental results on the frictional behaviour of many surfaces show that the friction force can be expressed as a function of the slip rate and the time of contact [2]. Moreover, for lubricated smooth surfaces, the viscous type regime crosses into the boundary regime of lubrication, or into a solid–solid type behaviour with a yield limit and irreversible displacements, by decreasing the film thickness [1]. These experimental observations have been taken into account by defining the friction force as a function of the sliding distance, the sliding rate and the average time of contact. Furthermore, the pure frictional and the pure viscous contribution to the friction force are weighted by means of a coefficient depending on the sliding velocity and the lubricated layer thickness. The beginning of sliding is defined with a Coulomb type yield function. For a steady state sliding, the yield threshold decreases exponentially with the sliding velocity until the dynamic friction value is reached. Based on stability conditions, it is assumed that the static friction coefficient increases slowly with the time of contact [2]. The model is formulated with respect to convective coordinates.

2 Thermodynamical framework

Considering the contact area Γ_c as a material boundary [3], the Clausius–Duhem inequality reads as

$$\mathcal{D} = t_N \dot{g} + \boldsymbol{t}_T \cdot \mathcal{L}_{\mathcal{V}} \boldsymbol{g}_T - \dot{\psi} \geq 0\,, \tag{1}$$

with ψ the surface free energy, t_N and $\boldsymbol{t}_T$ the normal and tangential component of the contact force, respectively, $\dot{g}$ the time derivative of the gap function, and $\mathcal{L}_{\mathcal{V}} \boldsymbol{g}_T$ the Lie derivative of the slip distance $\boldsymbol{g}_T$ [4].

Following Curnier [5], the total slip distance $\boldsymbol{g}_T$ is decomposed into an elastic and a permanent part $\boldsymbol{g}_T = \boldsymbol{g}_T^e + \boldsymbol{g}_T^p$, and so also $\boldsymbol{t}_T$, as $\boldsymbol{t}_T = \boldsymbol{t}_T^e + \boldsymbol{t}_T^i$, with $\boldsymbol{t}_T^e$ the elastic component and $\boldsymbol{t}_T^i$ the inelastic one.

3 Contact model for lubricated interface

Likewise for the formulation of a generalized standard material, the contact constitutive equations are derived from a free potential $\psi = \psi(g, \boldsymbol{g}_T; \boldsymbol{g}_T^p, \theta)$, with θ the average time of contact, and a dissipation potential $\phi = \phi(\mathcal{L}_{\mathcal{V}} \boldsymbol{g}_T, \mathcal{L}_{\mathcal{V}} \boldsymbol{g}_T^p, \dot{\theta})$ so that the inequality (1) holds. The corresponding state laws are written then as follows

$$t_N - K_N\, g \in \partial I_{x \geq 0}(g) \quad \Leftrightarrow g \geq 0\,, \quad (t_N - K_N g) g = 0\,, \quad t_N - K_N g \leq 0\,, \quad \boldsymbol{t}_T = (1-\alpha) K_T\, \boldsymbol{g}_T^e + \alpha \eta_b \mathcal{L}_{\mathcal{V}} \boldsymbol{g}_T\,, \tag{2}$$

where $\alpha \in [0,1]$, depends on $|\mathcal{L}_{\mathcal{V}} \boldsymbol{g}_T|$ and on the lubricant layer thickness D, K_N and K_T are penalty coefficients and η_b is the lubricant viscous parameter. The evolution laws are on the other hand given by

$$\mathcal{L}_{\mathcal{V}} \boldsymbol{g}_T^p = \lambda \frac{\boldsymbol{t}_T^e}{|\boldsymbol{t}_T^e|}\,, \quad \dot{\theta} = 1 - \theta \frac{|\mathcal{L}_{\mathcal{V}} \boldsymbol{g}_T|}{D_0}\,, \quad \text{with} \quad \mathcal{F} = |\boldsymbol{t}_T^e| - f(|\mathcal{L}_{\mathcal{V}} \boldsymbol{g}_T, \theta|) \mu_0(|\mathcal{L}_{\mathcal{V}} \boldsymbol{g}_T|) t_N \leq 0\,, \quad \lambda \mathcal{F} = 0\,, \quad \lambda \geq 0\,,$$

where λ is the plastic multiplier, D_0 can be interpreted as a memory distance over which the contact population changes, $\mathcal{F}$ is the sliding function and μ_0 is the steady state friction coefficient that decreases exponentially with the sliding velocity. The function $f(|\mathcal{L}_v \boldsymbol{g}_T|\,, \theta) = 1 + M \ln(\theta \frac{|\mathcal{L}_v \boldsymbol{g}_T|}{D_0})$ introduces the history of the sliding surface, resulting from creep of the surface contact with the consequent increase in the real contact area with time of contact.

From (2) it follows that for $\alpha = 0$ the rate–state variable Coulomb type behaviour is obtained, for $\alpha = 1$ the contact law is that of a Newtonian fluid with viscosity η_b, whereas for $\alpha \in (0,1)$ an intermediate behaviour is obtained.

* Corresponding author: e-mail: mluege@herrera.unt.edu.ar

4 Numerical example

An implicit Euler scheme with a predictor/corrector step is adopted for the numerical integration of the proposed model. The numerical implementation is done in the finite element code STAMPACK® [6]. The following example compares the numerical simulation of the pear–shaped tube expansion test with three different lubricants A, B, C and with no lubricant. Plane strain conditions with quadrilateral bilinear FEs are used, as shown in Figure $1(b)$. The stainless steel tube (SS304), with thickness $1.6mm$ and diameter $\phi = 57mm$ is modelled with von Mises elastoplasticity. Numerical results for the different tribological conditions using Coulomb friction law and the proposed model are compared in Figure $2(a)$ and Figure $2(b)$, respectively. It is clear that the proposed model is able to reproduce the experimental observations on the final wall thickness.

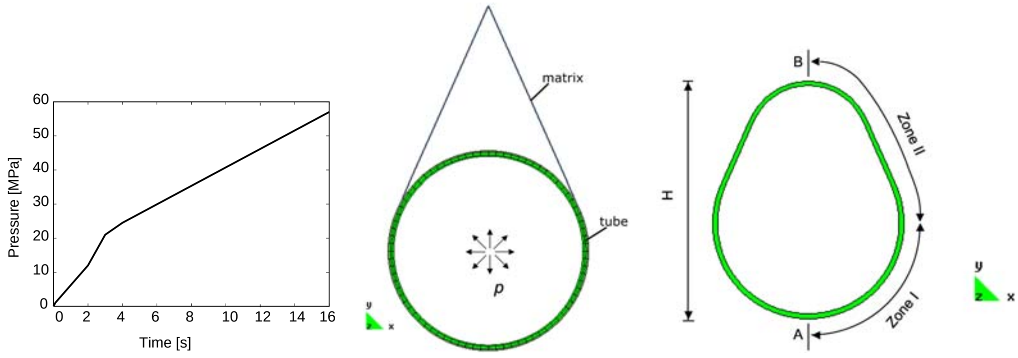

(a) (b) (c)

Fig. 1 Pressure–loading path used in the test for non burst specimens (a). Finite element model of the tube place in a pear–shape matrix under internal pressure p (b). Deformed specimen (c).

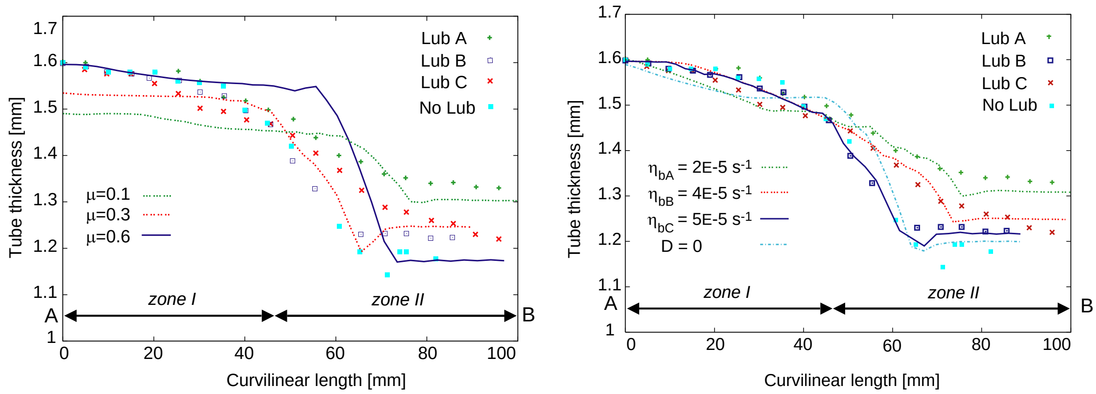

(a) (b)

Fig. 2 Effect of lubricants on the wall thickness distribution using the classical Coulomb friction law (a) and the proposed contact model (b), with $K_N = K_T = 2.0\,MPa/mm$, $M = 1.0 \cdot 10^{-1}$, $D_0 = 1.0 \cdot 10^{-3}\,mm$.

Acknowledgements This work has been supported by the CONICET

References

[1] G. Luengo, F.-J. Schmitt, R. Hill and J. Israelachvili. Thin film rheology and tribology of confined polymer melts: Contrasts with bulk properties. Macromolecules, **30**, 2482–2494 (1997).
[2] A.L. Ruina, Slip instability and state variable friction laws, Journal of Geophysical Research, **88**, 359–370 (1983).
[3] M. Fremond, Adhérence des solides, Journal de Mécanique Théorique et Appliquée, **6**, 383–407 (1987).
[4] T.A. Laursen, Computational Contact and Impact Mechanics, (Springer, Berlin, 2002).
[5] A. Curnier, A theory of friction, International Journal of Solids Structures, **20**, 637–647 (1984).
[6] STAMPACK®, Simulation software for multi-stage metal forming operations, Quantech, Barcelona, Spain.